IEEE Photonics Journal
An IEEE Photonics Society Publication

Open Access

Polarization-Modulation, I/Q-Demodulation Photonic Bandpass Sampling for Wideband, Multicarrier RF Application

Volume 9, Number 5, October 2017

Jieyu Ning
Yitang Dai
Feifei Yin
Junyi Zhang
Jianqiang Li
Wangzhe Li
Kun Xu

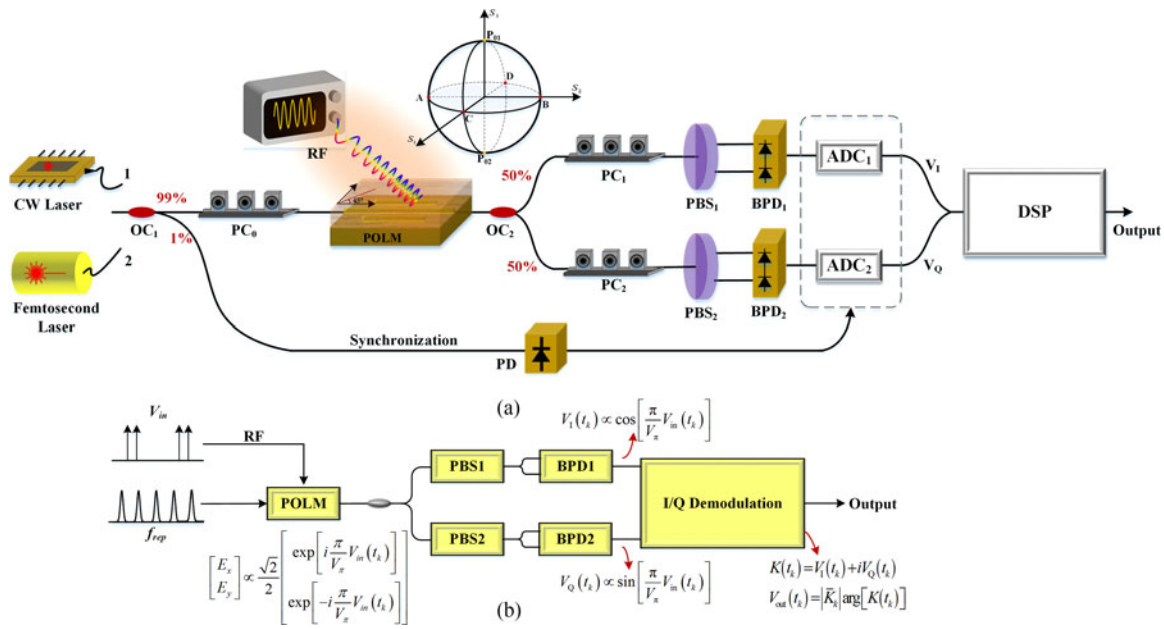

DOI: 10.1109/JPHOT.2017.2732918

Polarization-Modulation, I/Q-Demodulation Photonic Bandpass Sampling for Wideband, Multicarrier RF Application

Jieyu Ning,[1] Yitang Dai,[1] Feifei Yin,[1] Junyi Zhang,[2] Jianqiang Li,[1] Wangzhe Li,[3] and Kun Xu[1]

[1]State Key Laboratory of Information Photonics and Optical Communications, Beijing University of Posts and Telecommunications, Beijing 100876, China
[2]School of Electronic Engineering, Beijing University of Posts and Telecommunications, Beijing 100876, China
[3]National Key Lab of Microwave Imaging Technology, Institute of Electronics, Chinese Academy of Sciences, Beijing 100190, China
[4]School of Science, Beijing University of Posts and Telecommunications, Beijing 100876, China

DOI:10.1109/JPHOT.2017.2732918

Manuscript received June 6, 2017; revised July 19, 2017; accepted July 25, 2017. Date of publication July 27, 2017; date of current version August 14, 2017. This work was supported by the National Natural Science Foundation of China under Grant 61471065, Grant 61671071, and Grant 61625104.
Corresponding author: Yitang Dai (e-mail: ytdai@bupt.edu.cn).

Abstract: Radio frequency (RF) photonic link under phase or polarization modulation and coherent in-phase/quadrature (I/Q) demodulation (ΦM/IQ or PolM/IQ) has been reported with unprecedented dynamic range performance, benefiting from the ultrahigh linear transfer function of electro-optic phase modulator. But the ideal linear demodulation cannot be preserved during traditional down-conversion, which is a must from high-carrier application. In this paper, we propose and demonstrate that PolM/IQ link employing ultrashort optical bandpass sampling delivers both multicarrier down-conversion and full linearization. The pulse train, equivalently a frequency comb with uniform amplitude and phase in frequency domain, is able to down-convert signal and all nonlinear spurs that are collected by the following analog-to-digital convertor (ADC), so that the original linearization algorithm stands. Our method releases the requirement of ADC and digital processing greatly. The bandwidth after bandpass sampling is confined within the first Nyquist zone, and the minimum value can be as small as signal bandwidth, much less than original which should be several times of the maximum carrier frequency. We demonstrate such linearization experimentally with two dual-carrier RF signals as input, covering multiple octave spans.

Index Terms: Fiber optics links and subsystems, radio frequency (RF) photonics, analog optical signal processing.

1. Introduction

Radio frequency (RF) photonic link has been very attractive during the past years for both commercial and military applications, for example, antenna remoting [1], radio astronomy [2], 5G and beyond systems [3]. The spurious-free dynamic range (SFDR) is one of the most important parameters to evaluate the performance of a link. Though external modulation is widely adopted due to its simple structure, capacity for high speed, and commercial availability, its intrinsical nonlinear

transfer function, either in transmitter for Mach-Zehnder modulator (MZM) [4] or in receiver end for phase modulator [5], may introduce both harmonic crosstalk and intermodulation distortion, which deteriorates the link's dynamic range. Elimination of such nonlinear interfering is essential for high-quality links, which has been reported in previous literatures. In hardware the linearization has been reported by electronic pre-distortion [6], dual MZMs in parallel [7] or in series [8], optical phase-locked loop [9], bias-modulated photo detector (PD) [10], and so on. Recently the digital post distortion suppression by digital signal processing (DSP) has been demonstrated [11]–[14] and especially attractive due to its superior linearization ability and flexibility under link parameter dynamics. As a result, the optical down-conversion combined with DSP linearization has been considered as a promising strategy for remote RF receiving.

Many reported digital linearization schemes as well as algorithms serve the intensity-modulated and direct-detection (IMDD) RF photonic link due to its simple structure. Advanced approaches could linearize the target channel when several RF carriers co-exist, covering multiple octave spans, that is, both the third-order intermodulation distortion (IMD3) and the cross modulation distortion (XMD) could be suppressed simultaneously [15]–[17]. Other setups based on phase modulation, direct or coherent detection is similar to IMDD link, sharing the same mathematics [18], [19], so that the above digital processing still works. Note that with down-conversion, the traditional RF photonic link is actually a "filtered one" [20], [21]. Only the specific fundamental is digitalized, while other harmonic distortions are discarded. Such incomplete digitalization results in nonlinear transfer function deviation from standard sinusoidal, worsely, involving particular link parameters such as lightwave power, bias angle and half-wave voltage (V_π) of modulator, PD responsivity, etc. Consequently, almost all of the reported digital linearization schemes aim to eliminating the lowest-order same-frequency interfering, i.e., the IMD3. After the implementation, higher-order nonlinear spurs, ordinarily the fifth-order, limit the dynamic range [22], [23]. A full linearization then requires iteration [24], [25], which may increase the instability. Demodulation of phase encoded RF signal using coherent in-phase/quadrature (I/Q) detection, or ΦM/IQ, which benefits from the highly-linear phase modulation and digital I/Q demodulation, can solve the above problem in theory, by reversing digitally the link transfer function [26]. Such linearization is independent from any system variations (optical power, PD responsivity, etc.). In [14], we proposed polarization modulation with I/Q demodulation (PolM/IQ) in order to get rid of the demand of remote delivering a coherent optical local oscillation (LO).

However, there are still two unsolved problems of digital linearized ΦM/IQ or PolM/IQ RF photonic link. Firstly, full linearization requires digitalization of high-order harmonics, which results in largely wasteful analog-to-digital conversion (ADC) bandwidth as well as costly DSP operating. Even after down-conversion, the ADC bandwidth should be as large as several times of intermediate frequency (IF) carrier, much larger than the minimum signal bandwidth [26]–[28]. Secondly, the reported ΦM/IQ link with down-conversion cannot preserve the original perfectly-linear I/Q demodulation [26]–[28]. In order to down-convert high-order harmonics to within the ADC bandwidth, [26] employed a RF LO at approximately half the frequency of the RF signal to be converted. Since the quadratures suffer different conversion efficiency or phase shift, their digital synthesis is no longer precise reverse of link transfer function. As a result, only specific nonlinear spurs can be eliminated, similar to IMDD link.

In this paper, we propose that replacing the traditional down-conversion by ultra-short optical bandpass sampling, one can convert all orders of harmonics with uniform amplitude and phase, so that can preserve the original full linearization of a PolM/IQ link. Meanwhile, the required ADC bandwidth is compressed to the minimum value, that is, the signal bandwidth, without up re-sampling in the following digital implementation which also releases the requirement of DSP unit. We show in experiment that our scheme is capable of delivering multiple RF carriers, where several kinds of nonlinearities, including IMD3, XMD, and harmonic spurs, have been greatly suppressed.

2. Principle and Theoretical Analysis

The full linearization of ΦM/IQ or PolM/IQ RF photonic link relies on precisely collection of both in-phase and quadrature components, while each contains high-order harmonics, so that limited ADC

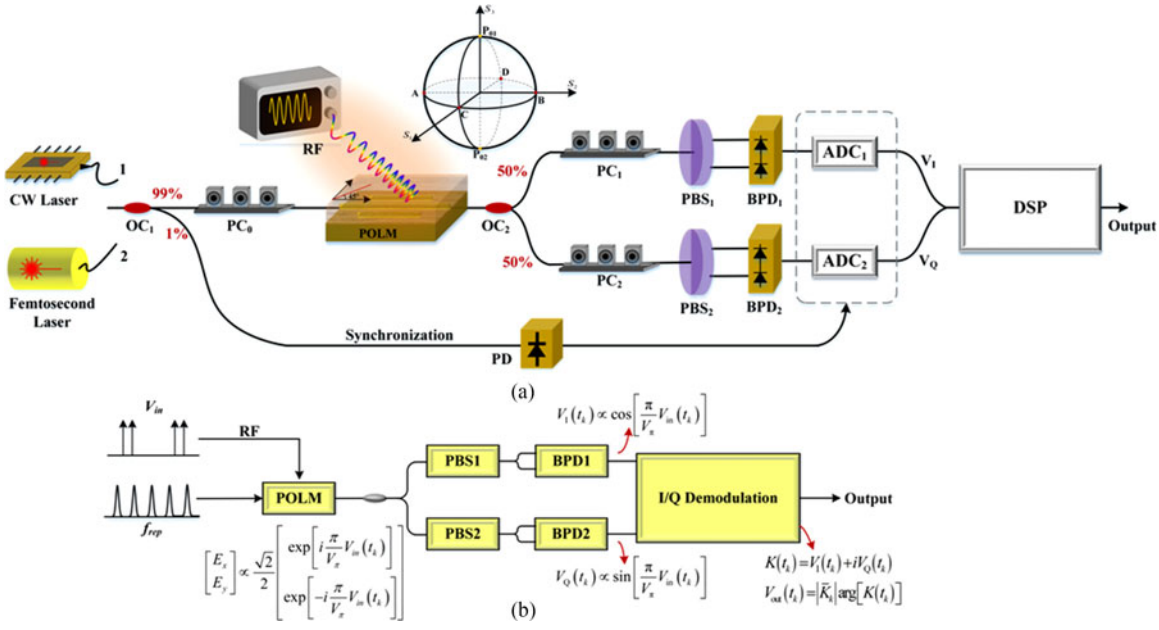

Fig. 1. Schematic diagram of the polarization-modulated optical bandpass sampling link.

bandwidth will result in residual nonlinear spurs. Such phenomenon is here studied numerically. The setup is shown in Fig. 1(a), where a linearly polarized continuous wave (CW) light is sent to a PolM, and its polarization state is rotated at an angle of 45° to one principal axis of the PolM using a polarization controller (PC_0). We assume that the two principle polarization states of PolM are perpendicular P_{01} and P_{02}, respectively, on the Poincare sphere. Then the incident lightwave is located on circle ACBD, and so is the polarization state after modulation, as shown in inset of Fig. 1(a). By PC_1, two output principles of a polarization beam splitter (PBS_1) are mapped to state A and B, respectively. The PBS converts polarization rotation into two complementary outputs and one can get the in-phase demodulation (V_I) through a balanced photo detector (BPD_1). Similarly, PC_2 maps PBS_2 to states C and D on the sphere and then one can get the quadrature demodulation (V_Q) after BPD_2. Both components are digitalized and numerically combined into complex quantity as $K = V_I + iV_Q$. The phase, arg(K), is then in theory proportional to analog voltage injected into PolM. In order to assign the regular unit to such dimensionless output, as well as to evaluate the link gain, we define the digital output as $\overline{|K|}\arg(K)$, where $\overline{|K|}$ is mean value of $|K|$. In simulation, we assume that the power of the CW lightwave is 12 dBm, the relative intensity noise (RIN) is -160 dBc/Hz, V_π of modulator is 5 V, the loss of PolM and other passive components is about 8 dB, and the PD responsivity is 0.9 A/W. A two-tone RF signal at 1 GHz is input, while the output electronic spectrum, the fundamental, and the intermodulation distortions are calculated, respectively. When the input RF power is 15 dBm per tone, the demodulated in-phase and quadrature components are shown individually in Fig. 2(a). Since the modulation depth is quite high, higher-order harmonics as large as 7 are stimulated. A full-bandwidth digitalization and following processing can result in perfect linearization. However, such bandwidth is far larger than signal passband. With a limited ADC bandwidth, the complementary of I/Q components no longer stands, and nonlinear spurs will occur after the above linearization algorithm. In Fig. 2(b), input RF power is varied from -10 to 15 dBm, and the powers of output fundamental and IMD3 are shown, when the ADC bandwidth is 1.5 GHz, 2.5 GHz, 3.5 GHz, and 4.5 GHz, respectively. When the bandwidth is compressed, the nonlinear spurs get increase significantly at a given input RF power. One can also observe that the IMD power changes along the input with different slope under different ADC. For example, when the bandwidth is 2.5 GHz, i.e., the 1st-order harmonic of quadrature and the 0th- and 2nd-order harmonics of in-phase component are considered, the slope is 5, which means the fifth-order intermodulation

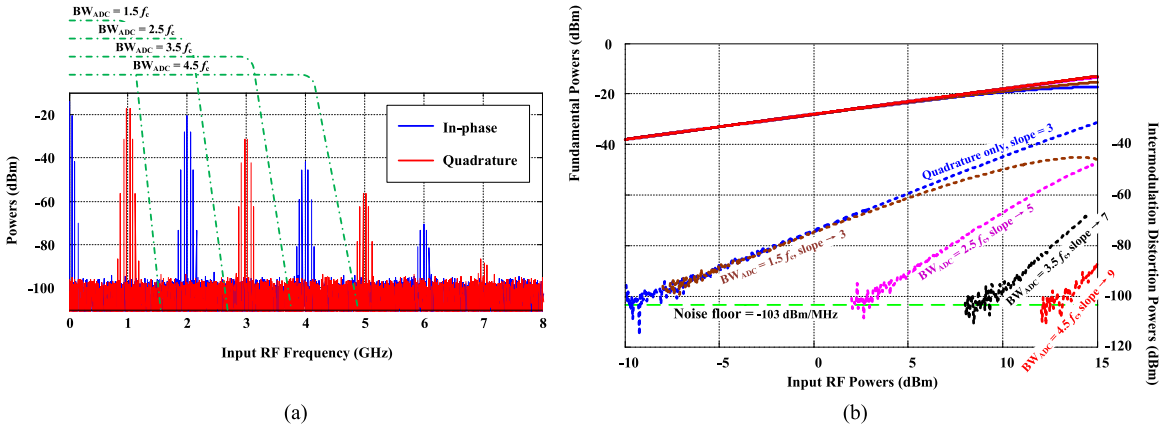

(a) (b)

Fig. 2. (a) The output electronic spectra of in-phase (the link transfer function is cos(.)) and quadrature (the link transfer function is sin(.)) components. The resolution bandwidth (RBW) is 1 MHz. BW_{ADC} is ADC bandwidth, and f_c is carrier frequency of input signal, which is 1 GHz. (b) The powers of output fundamental (solid lines) and IMD3 (dash lines) under different ADC bandwidth. In simulation we assume ADC resolution is high enough.

dominates nonlinearity and IMD3 is suppressed. This phenomenon has been widely reported in digitally-linearized IMDD link [22]. Actually the limited ADC bandwidth is equivalent to small-input-signal assumption where high-order nonlinearity is ignored. As a result, such spurs will appear when high voltage is applied on modulator.

In this paper, we replace the CW lightwave by a femtosecond fiber laser, as shown in Fig. 1(a), where the ADC is synchronized by the optical pulse train. Such implementation has two advantages. Firstly, down-conversion is obtained without frequency-variable electronic LO when signal carrier spans large frequency range. Multiple carriers may also be down-converted and distinguished in the first Nyquist zone simultaneously, which has not been reported in previous PM/IQ or PolM/IQ link. Secondly, according to [29], as long as the pulse duration is short enough, the photonic link with ADC in Fig. 1(a) is equivalent to a digital PolM/IQ link after bandpass discretization of input signal. The counterpart is shown in Fig. 1(b): the RF wave is first sampled by ideal impulse train, and then the generated discrete data, with the same repetition rate as the femtosecond fiber laser as well as other physical properties like polarization and pulse energy, pass through the PolM and I/Q demodulation. Sharing the same mathematics as a real link, the equivalent one delivers RF signal following equations shown in Fig. 1(b). The linearization algorithm is then

$$\begin{aligned} K\left(t_k\right) &= V_{\mathrm{I}}\left(t_k\right) + iV_{\mathrm{Q}}\left(t_k\right) \\ V_{\mathrm{out}}\left(t_k\right) &= \left|\bar{K}_k\right| \arg\left[K\left(t_k\right)\right] \end{aligned} \tag{1}$$

Compared with original continuous I/Q linearization, the discrete one described by (1) saves power of ADC and DSP greatly. Assume the repetition rate of femtosecond pulse train is f_{rep}. After the first-stage bandpass sampling, the bandwidth of input signal is limited within $[-f_{rep}/2, f_{rep}/2]$, so that the original wideband linearization can be obtained in such narrow digital baseband. Actually the above linearization is always effective no matter how large the signal bandwidth is. However, if the input bandwidth is larger than the Nyquist zone, the output will be compressed (the so-called compressive sampling).

Different from continuous case, our discrete PolM/IQ link does not need extra ADC/DSP bandwidth for high-order harmonics. In frequency domain, the femtosecond optical pulse train shows strictly-equally-spaced frequency comb lines, and all harmonics of both in-phase and quadrature components are down-converted into the first Nyquist zone by their neighbor lines, which are then collected by ADC. Such batch of frequency conversions shows advantage over [14], since the comb lines have much more uniform power and phase distribution than that driven by a phase modulator. Besides, all frequency-folded harmonics share the same bandwidth, which compress the ADC

TABLE 1
Mixtures of the Output Wideband RF Signal

Nonlinear Distortion	*The possible major distortions and harmonics*
Second-order mixtures	$2f_{11}$ $2f_{12}$ $2f_{22}$ $2f_{21}$ $f_{21}-f_{11}$ $f_{22}-f_{11}$ $f_{11}+f_{12}$ $f_{22}-f_{12}$ $f_{21}-f_{12}$ $f_{21}+f_{22}$
Third-order intermodulation distortion	$f_{21}-2f_{11}$ $2f_{22}-f_{11}$ $f_{21}-2f_{12}$ $2f_{21}-f_{12}$ $f_{22}-2f_{11}$ $2f_{22}-f_{12}$ $f_{22}-2f_{12}$ $2f_{21}-f_{11}$ $2f_{11}-f_{12}$ $2f_{12}-f_{11}$ $2f_{22}-f_{21}$ $2f_{21}-f_{22}$ $f_{21}-f_{11}-f_{12}$ $f_{21}+f_{22}-f_{11}$ $f_{22}-f_{11}-f_{12}$ $f_{21}+f_{22}-f_{12}$
Third-order harmonics distortion	$3f_{11}$ $3f_{12}$ $3f_{21}$ $3f_{22}$ $2f_{11}+f_{12}$ $2f_{11}+f_{21}$ $2f_{11}+f_{22}$ $2f_{12}+f_{11}$ $2f_{12}+f_{21}$ $2f_{12}+f_{22}$ $2f_{21}+f_{11}$ $2f_{21}+f_{12}$ $2f_{21}+f_{22}$ $2f_{22}+f_{11}$ $2f_{22}+f_{12}$ $2f_{22}+f_{21}$ $f_{12}+f_{21}+f_{22}$ $f_{11}+f_{21}+f_{22}$ $f_{11}+f_{12}+f_{22}$ $f_{11}+f_{12}+f_{21}$
Third-order cross-modulation distortion	$f_{11}+f_{21}-f_{22}$ $f_{11}+f_{22}-f_{21}$ $f_{12}+f_{21}-f_{22}$ $f_{12}+f_{22}-f_{21}$ $f_{11}+f_{21}-f_{12}$ $f_{21}+f_{12}-f_{11}$ $f_{11}+f_{22}-f_{12}$ $f_{22}+f_{12}-f_{11}$

bandwidth further to its minimum value, that is, the signal bandwidth. Note that in order to approach the above theoretical equivalence and perfect linearization, the optical pulse should be so short that its comb lines cover sufficient nonlinear harmonics. Fig. 2(b) shows that harmonics higher than 5th order are neglectable since the nonlinear spurs to be suppressed may be under noise floor in the specific example. As result, the optical pulse should be short enough to bandpass sample five times of the maximum input carrier frequency. Such requirement can be easily achieved by current femtosecond fiber laser: the pulse duration is much less than 1 ps which can support bandpass sampling of harmonics of microwaves.

3. Experimental Results and Discussion

The experiment follows the setup shown in Fig. 1(a) where the optical source is a femtosecond fiber laser. The laser (ELMO from MenloSystems, Inc.) has a repetition of 100.05958 MHz, and the average output power is around 12 dBm. Approximately 1% of the optical power is tapped off directly and opto-electronically converted by a low-speed PD to synchronize the electronic ADC. The other part of optical pulses is used to sample the RF signal via PolM. The PolM is a single AlGaAs-GaAs mode-converter-based polarization modulator with 40 GHz electrical bandwidth. In our setup we use three PCs to ensure the required full-scale polarization modulation and the optimal conversion to I/Q demodulation. The average optical power before the second 1:1 optical coupler is 8.47 dBm. Baseband outputs from two home-made BPDs are acquired simultaneously by a dual-channel ADC (from ADLink with 14-bit level, and the maximum sampling rate is 200 MSamples/s). The bandwidth of our BPDs is 3 GHz. Time delay mismatch between I and Q paths is corrected in digital domain. The linearization algorithm is realized by an offline MATLAB program. Here the PolM is driven by two dual-tone RF signals, noted as S_A and S_B, respectively, in order to verify our linearization not only for regular IMD3 but also for nonlinear spurs stimulated by multiple carriers. S_A is at 1.511 GHz (f_{11}) and 1.513 GHz (f_{12}), separately, and S_B is at 10.041 GHz (f_{21}) and 10.0405 GHz (f_{22}). The two dual-tone signals are separated far away from each other in order to demonstrate the ultra-broadband capacity of our proposal. For the wideband optical link, the possible major distortions and harmonics are governed by $[\cos(2\pi f_{11}t)+\cos(2\pi f_{12}t)+\cos(2\pi f_{21}t)+\cos(2\pi f_{22}t)]^k$, $k = 2, 3\ldots$ The frequencies of major spurs ($k = 2, 3$) are shown in Table 1. We here classify the nonlinear spurs into four groups: (1) the second-order mixtures, (2) the third-order intermodulation distortion (including both internal IMD3 and external IMD3), (3) the third-order harmonics (i.e., the

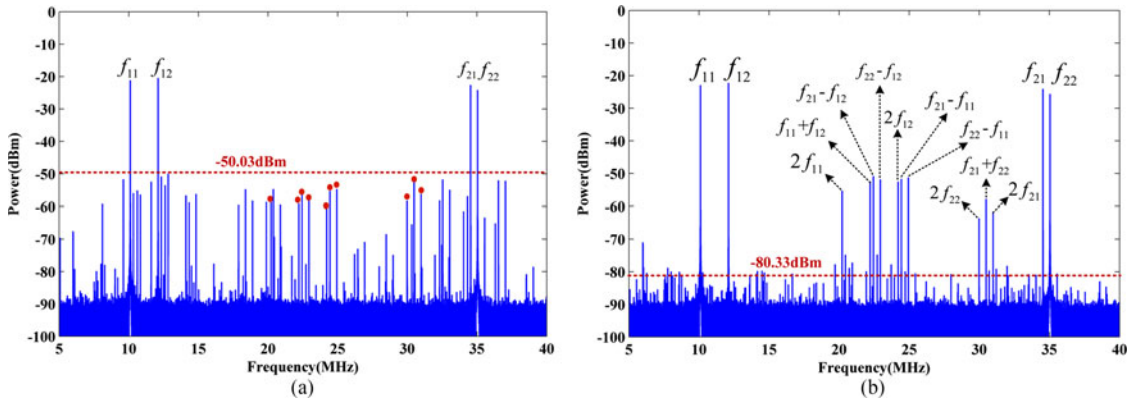

Fig. 3. Output spectrums of the down-converted multi-carrier signal for the bandpass sampled RF optical link (a) when only the quadrature component is considered and (b) when the I/Q demodulation is performed. The red points represent the residual 2^{nd}-order distortions.

sum-frequency spurs of any three of the four tones), and (4) the third-order cross-modulation, which is induced by the modulation from the other signal.

When the powers of the four sinusoidal waves are all 3.5 dBm at the PolM, the received IF signal of the quadrature component only (where the PC_2 is optimized so that the corresponding transfer function is sin(·)) and of the I/Q linearization are shown in Fig. 3(a) and (b), respectively. As can be seen, S_A is down-converted to 10.1 MHz and 12.1 MHz, while the IF signal corresponding to S_B is 34.54 MHz and 35.04 MHz. All distortions listed in Table 1 can be found in the first Nyquist zone, and one can observe in Fig. 3(a) that the average power of the nonlinear spurs is about −50 dBm. The internal IMD3 and XMD are usually considered in single- or multi-carrier link since they cover the same band as the received signals. The 3rd-order harmonics and external IMD3 are usually out of the signal band, but have to be included in multi-octave-span scenario. All the 3rd-order nonlinearities share almost the same major significance, so that the elimination of all is a must. After linearization based on (1), the 3rd-order spurs power is about −80 dBm in Fig. 3(b), 30 dB less than the original. Note that there are still significant nonlinear spurs left after the linearization, which are the residual 2nd-order distortions. We believe such spurs result from the amplitude-modulation-to-phase-modulation (AM-PM) conversion, which is a kind of nonlinearity of PD [30]. Since the phenomenon has not been considered in current numerical link model, the 2nd-order distortions have not been corrected.

Fig. 4 shows the suppression ratios of the fundamental sidebands to the XMD sidebands of two signals. When the power of S_B applied on the PolM is fixed at 3 dBm, the power of S_A is scanned from 0 dBm to 3.5 dBm. The received down-converted fundamental sidebands and XMD sidebands of S_B are measured, and the suppression ratios are plotted in Fig. 4(a). As can be seen the XMD sidebands are well suppressed by 28 dB. Similarly, when the power of S_A is kept unchanged at 3 dBm, the power of S_B varies from 0 dBm to 3.5 dBm, the received down-converted fundamental sidebands and XMD sidebands of S_A are recorded, and the 30.4 dB-suppression is experimentally illustrated in Fig. 4(b).

Furthermore, Fig. 5 shows the detected down-converted power of the fundamental and the internal IMD3 as a function of the input RF powers for both cases with and without digital linearization. Scanning the input signals S_A and S_B from 0 dBm to 3.5 dBm, the received powers of the fundamental and IMD3 tones are recorded. It is obvious to see that the SFDRs of the two RF signals are both improved. Ignoring the digitalization noise from ADC, the measured noise floor after BPD is −167.3 dBm/Hz. The SFDR of the input signal S_A before and after the linearization is 111.3 dBm·$Hz^{2/3}$ and 118.7 dBm·$Hz^{2/3}$, respectively, while the SFDR of the input signal S_B after the linearization is 118.1 dBm·$Hz^{2/3}$. We note that the current design is still limited by the quantization noise of the ADC. Such limitation is expected to be removed by a low-noise linear electronic amplifier before the ADC [31].

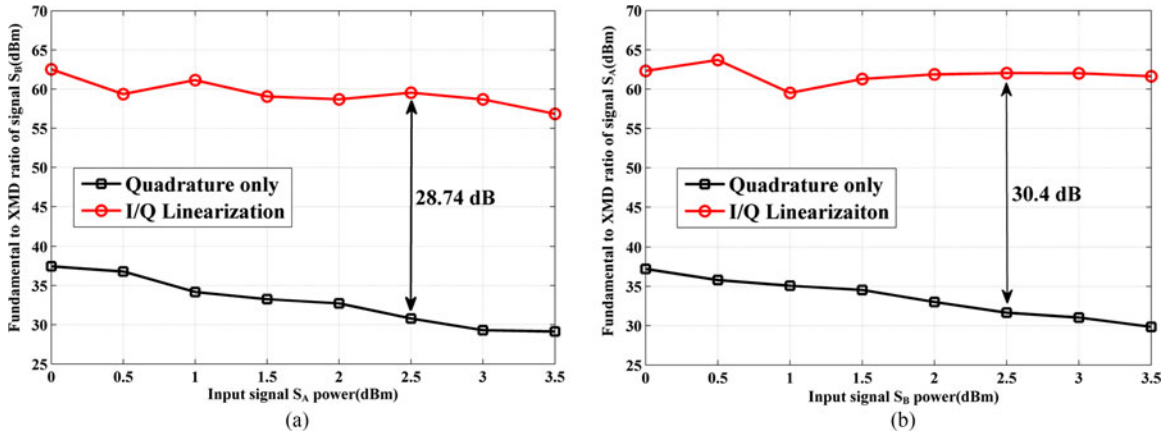

Fig. 4. (a) The ratios of the received fundamental to XMD sidebands of S_B with the varying powers of S_A and (b) the ratios of the received fundamental to XMD sidebands of S_A with the varying powers of S_B for both cases that only the quadrature component and the I/Q demodulation are performed.

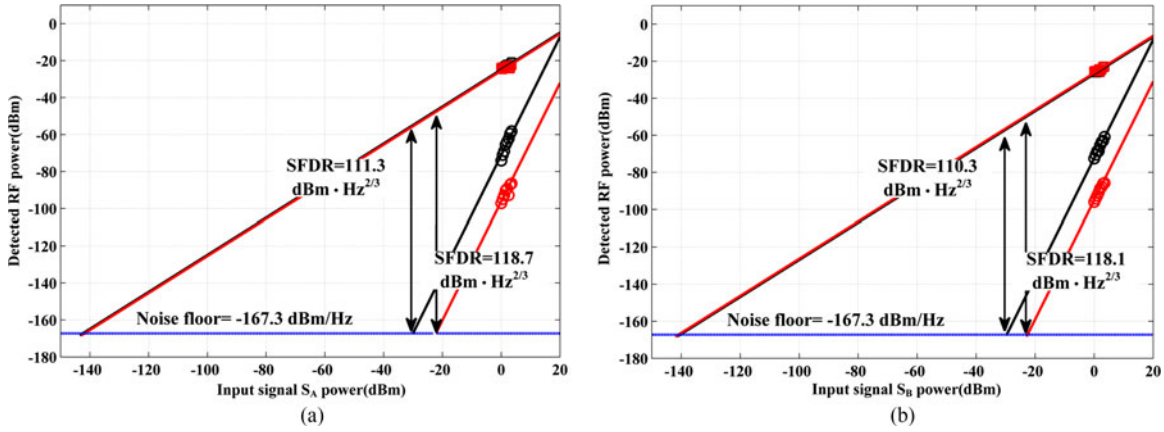

Fig. 5. Measured down-converted IF and internal IMD3 components versus the input RF power without and with the proposed digital linearization. (a) for S_A and (b) for S_B.

4. Conclusion

In conclusion, we have proposed and experimentally demonstrated a novel photonic-bandpass-sampled, polarization-modulated RF link with I/Q demodulation, which is capable of multi-carrier down-conversion and digital linearization of multiple co-exist nonlinear spurs. Though with traditional PolM/IQ setup, the ultra-short sampling ensures collecting and processing all orders of nonlinearity, and the required digital bandwidth is compressed to the minimum value. Experimentally, we input two dual-tone RF signals under 1.5 GHz and 10 GHz, respectively, and observed 30-dB suppression of multiple nonlinear spurs after down-conversion. The dynamic ranges of target IF signals were both 118 dBm·Hz$^{2/3}$. This, to the best of our knowledge, is the first time to demonstrate a down-converted PolM of PM photonic link that preserves the original linear I/Q demodulation. Our approach may benefit future wideband, multi-carrier RF applications.

References

[1] J. Yao, "Microwave photonics," *J. Lightw. Technol.*, vol. 27, no. 3, pp. 314–335, Feb. 2009.
[2] W. Shieh *et al.*, "Performance of a 12-kilometer photonic link for X-band antenna remoting in NASA's deep space network," *Telecommun. Mission Oper. Prog. Rep.*, vol. 138, pp. 1–8, 1999.

[3] R. Waterhouse and D. Novak, "Realizing 5G: Microwave photonics for 5G mobile wireless systems," *IEEE Microw. Mag.*, vol. 16, no. 8, pp. 84–92, Sep. 2015.
[4] E. I. Ackerman, "Broad-band linearization of a Mach-Zehnder electro-optic modulator," *IEEE Trans. Microw. Theory Techn.*, vol. 47, no. 12, pp. 2271–2279, Dec. 2000.
[5] A. Caballero, D. Zibar, I. T. Monroy, "Performance evaluation of digital coherent receivers for phase-modulated radio-over-fiber links," *J. Lightw. Technol.*, vol. 29, no. 21, pp. 3282–3292, Nov. 2011.
[6] V. J. Urick, M. S. Rogge, P. F. Knapp, L. Swingen, F. Bucholtz, "Wide-band predistortion linearization for externally modulated long-haul analog fiber-optic links," *IEEE Trans. Microw. Theory Techn.*, vol. 54, no. 4, pp. 1458–1463, Jun. 2006.
[7] S. K. Korotky and R. M. Ridder, "Dual parallel modulation schemes for low distortion analog optical transmission," *IEEE J. Sel. Areas Commun.*, vol. 8, no. 7, pp. 1377–1381, Sep. 1990.
[8] D. J. M. Sabido, M. Tabara, T. K. Fong, C. L. Lu, L. G. Kazovsky, "Improving the dynamic range of a coherent AM analog optical link using a cascaded linearized modulator," *IEEE Photon. Technol. Lett.*, vol. 7, no. 7, pp. 813–815, Jul. 1995.
[9] D. Zibar *et al.*, "Dynamic range enhancement of a novel phase locked coherent optical phase demodulator," *Opt. Exp.*, vol. 15, no. 1, pp. 33–44, 2007.
[10] F. Yin *et al.*, "Dynamic range improvement in analog photonic link by intermodulation-compensation receiver," *Opt. Exp.*, vol. 23, no. 9, pp. 11242–11249, 2015.
[11] A. Fard *et al.*, "Digital broadband linearization technique and its application to photonic time-stretch analog-to-digital converter," *Opt. Lett.*, vol. 36, no. 7, pp. 1077–1079, 2011.
[12] T. R. Clark and M. L. Dennis, "DSP-based highly linear microwave photonic link," in *Proc. IEEE/MTT-S Int. Microw. Symp.*, 2007, pp. 1507–1510.
[13] T. R. Clark, T. R., M. Currie, P. J. Matthews, "Digitally linearized wide-band photonic link," *J. Lightw. Technol.*, vol. 19, no. 2, pp. 172–179, 2001.
[14] Q. Lv *et al.*, "I/Q intensity-demodulation analog photonic link based on polarization modulator," *Opt. Lett.*, vol. 36, no. 23, pp. 4602–4604, 2011.
[15] A. Agarwal, T. Banwell, P. Toliver, T. K. Woodward, "Predistortion compensation of nonlinearities in channelized RF photonic links using a dual-port optical modulator," *IEEE Photon. Technol. Lett.*, vol. 23, no. 1, 2011.
[16] X. Xie *et al.*, "Digital nonlinearities compensation based on forward distortion information acquisition in channelized RF photonic links," in *Proc. Int. Topical Meet. Microw. Photon.*, 2012, pp. 88–91.
[17] X. Liang *et al.*, "Digital suppression of both cross and inter-modulation distortion in multi-carrier RF photonic link with down-conversion," *Opt. Exp.*, vol. 22, no. 23, pp. 28247–28255, 2014.
[18] R. Li, X. Han, X. Chen, X. Chen, J. Yao, "A phase-modulated microwave photonic link with an extended transmission distance," *IEEE Photon. Technol. Lett.*, vol. 27, no. 24, pp. 2563–2566, Dec. 2015.
[19] H. Yu *et al.*, "Photonic down-conversion and linearization of microwave signal from the X- to K-band," *IEEE Photon. Technol. Lett.*, vol. 27, no. 19, pp. 2015–2018, Oct. 2015.
[20] A. Agarwal, T. Banwell, T. K. Woodward, "Optically filtered microwave photonic links for RF signal processing applications," *J. Lightw. Technol.*, vol. 29, no. 16, pp. 2394–2401, Aug. 2011.
[21] T. Banwell *et al.*, "Analytical expression for large signal transfer function of an optically filtered analog link," *Opt. Exp.*, vol. 17, no. 18, pp. 15449–15454, 2009.
[22] Y. Cui *et al.*, "Enhanced spurious-free dynamic range in intensity-modulated analog photonic link using digital post-processing," *IEEE Photon. J.*, vol. 6, no. 2, Apr. 2014, Art. no. 7900608.
[23] F. Yin *et al.*, "Wide-band RF photonic link based on analog linearization," in *Proc. Asia Commun. Photon. Conf.*, 2015, Paper ASu1J.4.
[24] A. Fard *et al.*, "Digital broadband linearization technique and its application to photonic time-stretch analog-to-digital converter," *Opt. Lett.*, vol. 36, no. 7, pp. 1077–1079, 2011.
[25] X. Liu *et al.*, "Suppression of nonlinear distortions in intensity modulated analog photonic link employing digital signal post-processing," in *Proc. Int. Topical Meet. Microw. Photon.*, 2016, pp. 129–132.
[26] T. R. Clark, S. R. O'Connor, M. L. Dennis, "A phase-modulation I/Q-demodulation microwave-to-digital photonic link," *IEEE Trans. Microw. Theory Techn.*, vol. 58, no. 11, pp. 3039–3058, Nov. 2010.
[27] T. R. Clark and M. L. Dennis, "Linear microwave downconverting RF-to-bits link," in *Proc. IEEE Int. Topical Meet. Microw. Photon. Asia-Pacific Microw. Photon. Conf.*, 2008, pp. 12–14.
[28] T. R. Clark and M. L. Dennis, "Coherent optical phase-modulation link," *IEEE Photon. Technol. Lett.*, vol. 19, no. 16, pp. 1206–1208, Aug. 2007.
[29] Y. Dai *et al.*, "Digital linearization of multi-carrier RF link with photonic bandpass sampling," *Opt. Exp.*, vol. 23, no. 18, pp. 23177–23184, 2015.
[30] X. Liang *et al.*, "Amplitude modulation to phase distortion conversion in photonic bandpass sampling link," in *Proc. IEEE Avionics Vehicle Fiber-Opt. Photon. Conf.*, 2016, pp. 203–204.
[31] Y. Dai *et al.*, "Performance improvement in analog photonics link incorporating digital post-compensation and low-noise electrical amplifier," *IEEE Photon. J.*, vol. 6, no. 4, Aug. 2014, Art. no. 5500807.